Progress in Theoretical and Applied Physics
Vol. 1, 2013, 17-31
ISSN: 2320-3064 (Print) , 2320-3072 (Online)
Published on 31 January 2013
www.researchmathsci.org

Progress in
Theoretical and Applied Physics

Structural and Morphological Characterization of ZnO thin Films Synthesized by SILAR

P. Mitra and S. Mondal

Department of Physics, The University of Burdwan, Burdwan 713104, India
Email: mitrapartha1@rediffmail.com

Received 31 August 2012; accepted 1 October 2012

Abstract. Zinc oxide (ZnO) thin films were deposited on glass substrates from ammonium zincate complex as cationic precursor following SILAR (Successive ion layer adsorption and reaction) technique. Characterization techniques of XRD, HRSEM, TEM, EDX and FTIR were utilized for detailed microstructural studies of the coated films. A comparison of physical properties of the films was made from those deposited from other zinc complexes as cationic precursor. Particle size analysis using x-ray line broadening analysis shows an average particle of 22.75 nm for ZnO film. Both instrumental and strain broadening was taken into account while estimating the particle size. The value agrees well with 25.8 nm obtained from TEM measurement. Films are highly c-axis oriented with a texture coefficient value of ~2.29 for (002) plane. EDX spectrum indicates that the film consist of zinc and oxygen elements. The characteristic stretching vibration mode of ZnO was observed in the absorption band in FTIR spectrum. Film with best homogeneity, compactness, highest c-axis orientation and least crystallite size was obtained from ammonium zincate complex.

Keywords: ZnO thin films, SILAR, XRD, TEM, Particle size

1. Introduction

ZnO is one of the most important II-VI wide band gap (WBG) semiconducting material with a bandgap of around 3.2-3.37eV at room temperature 300K. Besides being a WBG material, it has several other advantages. Some of the favorable aspects of ZnO include its radiation hardness, biocompatibility and its high transparency in visible region. ZnO is important for its multi-functional properties (semiconducting, magnetic, piezoelectric etc.) for electronic and optoelectronic devices. Among different physical forms, the thin films of ZnO find a multitude of immensely important applications in electronic and optoelectronic devices such as transparent conductors, solar cell windows, gas sensors, surface acoustic wave (SAW) devices, heat mirrors etc. [1-2]. It is also being considered as a potential candidate in the new frontiers of research like spintronics.

Different techniques such as pulsed laser deposition, sputtering, thermal evaporation, condensation, solid state reaction and chemical methods have been employed to fabricate thin films of ZnO [3]. Chemical techniques involving aqueous route are relatively simpler and cost effective. However, for an extensive use in the commercial applications pure ZnO films must be prepared by a low temperature deposition methodology. Therefore, it is necessary to develop a low temperature deposition technology for the growth of ZnO films. In this study, ZnO thin films were synthesized using successive ionic layer adsorption and reaction (SILAR) technique. Advantages of SILAR are effectiveness and simplicity of the deposition equipment, controlled deposition rates, wide spectrum of deposition parameters for the control and the optimization of film properties, and film thickness. SILAR is a wet chemical route for the synthesis of thin films in which the basic building blocks are ions instead of atoms and therefore the preparative parameters are easily controllable. The SILAR method, also known as modified version of chemical bath deposition, has a number of advantages apart from it being inexpensive, simple and convenient for large scale deposition: i) the process can be carried out on any kind of substrate, ii) unlike closed vapor deposition method, SILAR does not require high quality target and/or substrates. Also it does not require vacuum at any stage, iii) the deposition rate and the thickness of the film can be easily controlled by changing the deposition cycles, iv) it is a low temperature chemical solution method and does not cause local over heating that can be detrimental for materials to be deposited.

The SILAR method is basically a two-step chemical bath deposition technique in which a substrate is dipped in cationic and anionic precursors. The technique is thus based on the adsorption and reaction of the ions from the solutions. Sequential reaction on the substrate surface under optimized conditions of concentration and pH of the reacting solutions results in the formation of the film. Preparation of undoped ZnO thin films are performed using a zinc complex solution as first dip and a dip in hot water bath kept near boiling point as the second dip [4-5]. Although there are several efforts around on SILAR, it remains a less utilized technique for synthesis of pure ZnO thin film and their detailed characterization. For pure ZnO thin film deposition, the process was originally reported as multiple chemical dipping technique by Ristov et al [4]. It was ascribed with the name SILAR by Nicolau et al. [5] since it involves adsorption of a layer of complex ion on the substrate followed by reaction of the adsorbed ion layer. Several zinc complexes such as sodium zincate, zinc chloride, ammonium zincate prepared from zinc sulphate as starting precursor has been utilized as cationic precursors for ZnO film deposition using SILAR [4-9]. In this study synthesis of ZnO film was made from ammonium zincate complex prepared from zinc acetate dihydrate $\left[Zn\left(CH_3COO\right)_2 2H_2O\right]$ as the starting reagent for the first time. Microstructural characterization of the films has been studied and a comparison of physical properties has been made with ZnO films deposited from other zinc complex as cationic precursors Zinc acetate has a number of distinctive properties. It is known to be a ‘mono- precursor’ [10]. Also the ammonium acetate formed during its reaction with ammonia is highly soluble in water which reduces the possibility of impurity incorporation in the deposited films. Ammonium acetate is also a

relatively unusual example of a salt that melts at low temperatures. The coated films have been characterized by different techniques such as X-ray diffraction (XRD), Transmission Electron Microscopy (TEM), High Resolution Scanning Electron Microscopy (HRSEM), energy dispersive x-rays (EDX) and Fourier transform IR (FTIR) spectroscopy.

2. Experimental Details

Zinc oxide thin films were deposited on glass substrates (microscope slides) by alternate dipping into ammonium zincate $\left[\left(NH_4\right)ZnO_2\right]$ bath kept at room temperature and hot water maintained near boiling point. The ammonium zincate bath was prepared by adding ammonium hydroxide (~25% pure ammonia solution, density 0.91, Merck) to an aqueous solution of analytical grade zinc acetate dihydrate supplied by Merck. Ammonia solution was introduced slowly under continuous stirring until the solution becomes clear and homogeneous. An excess of alkali is always required to have a stable ammonium zincate bath [8, 11]. The glass substrate was cleaned, before deposition, by chromic acid followed by distilled water rinse and ultrasonic cleaning with acetone and alcohol. The reaction leading to the formation of ammonium zincate can be written as

$$Zn\left(CH_3COO\right)_2 + 4NH_4OH = \left(NH_4\right)_2 ZnO_2 + 2CH_3COONH_4 + 2H_2O$$

The precleaned substrate was immersed in the zinc complex for a known standardized time followed by immersion in hot water for the same time for hydrogenation. The film thickness was determined by weight difference-density consideration [12] method using an electronic high-precision balance. A check of this thickness was made by measuring the thickness using cross-sectional SEM.

The crystal structure and orientation of the ZnO films were investigated by X-ray diffraction (XRD) method employing a Philips PW 1830 x-ray diffractometer using Ni filtered CuK_α radiation (λ=1.5418 Å). The diffractometer reflection was taken at room temperature. Transmission electron microscopy (TEM) was used to study the surface morphology and to illustrate the formation of crystallites. The film was scratched from the surface prior to TEM measurements. EDX measurement was done to study the composition of the film and FTIR measurement was carried out to obtain information about the chemical bonding. A comparison of physical characteristics of the films obtained from ammonium zincate complex was made with those deposited from sodium zincate complex and zinc chloride solution as cationic precursors.

3. Results and discussions

3.1. Film deposition and thickness measurement

The substrate was first dipped in ammonium zincate bath kept at room temperature during which the substrate surface was covered with a thin layer of the complex zinc solution. During second immersion in hot water bath maintained near boiling point, the absorbed zinc complex is converted into ZnO. The dipping time in each bath was 2 seconds. This cycle was repeated several times in order to increase the overall film thickness. It is to mention that the ammonium zincate bath used for

deposition contains ammonium acetate as well. While the zincate precipitates as ZnO in presence of high concentration of water when dipped in hot water bath the acetate goes into the solution due to its high solubility in water. Use of sodium zincate bath instead of ammonium zincate bath as cationic precursor always introduces the possibility of incorporation of highly mobile sodium ions in the film, which can be detrimental for their practical applications [13]. The reaction occurring on the surface of the substrate leading to the formation of ZnO from ammonium zincate may be represented as:

$$\left(NH_4\right)_2 ZnO_2 + H_2O = ZnO + 2NH_4OH$$

The detailed chemical reaction involving zinc amine complex may be quite complicated. The presence of tetraamminezinc (II) $\left[Zn\left(NH_3\right)_4\right]^{2+}$ in presence of an excess ammonical solution has been reported by Jimenez-Gonzalez et al [7]. Thus the reaction scheme may be represented as:

$$\left[Zn\left(NH_3\right)_4\right]^{2+} + 4H_2O \rightarrow Zn^{2+} + 4NH_4{}^{+}OH^{-}$$

$$Zn^{2+} + 2OH^{-} \rightarrow Zn(OH)_2$$

Since the reaction temperature is close to the boiling point of water, zinc hydroxide breaks to give zinc oxide:

$$Zn(OH)_2 \rightarrow ZnO + H_2O$$

Thus some amount of zinc hydroxide is always present in the as deposited film [4, 6, 8]. The deposited film was subsequently annealed in air at different temperature.

The formation of the film was found to be a stringent function of zincate bath pH. Films produced with pH<10.7 was found to consists of non-adherent powder like precipitates indicating poor quality of deposition. The bath solution also tends to lose stability for pH<10.7. The ammonium zincate bath was found to be stable for pH values ≥ 10.7. However, above pH 10.9, the growth rate decreases abruptly. At very high pH value, it appears that dissolution of already deposited ZnO film occurs, when reintroduced into the solution. Thus the pH value was optimized maintained in the range 10.75-10.85 with a minimum of ammonia addition to get significant growth rate and good quality adherent films. The film thickness and growth process also depends on concentration of zinc complex. It was found that above 0.15M concentrations, particulate adsorption took place on the film surface making the growth process nonuniform and resulting in a poor quality film. The solution concentration was optimized at 0.1M to get good quality adherent films with a reasonable growth rate. Lower concentration reduces the growth rate of the film in a linear proportion.

The film thickness could be varied by varying the number of dipping. A linear increase in thickness with a growth rate of 0.016 μm per dipping was observed in the present experiment. The film thickness was also checked against cross-sectional SEM. Figure 1 shows the cross-sectional SEM micrograph of ZnO film of thickness 2.0 μm measured gravimetrically (obtained by 125 dipping). An average thickness of 2.64 μm was obtained from SEM micrograph. The value was

an average of several measurements on different portions of the film. This indicates a porosity of ~ 32% in the deposited films.

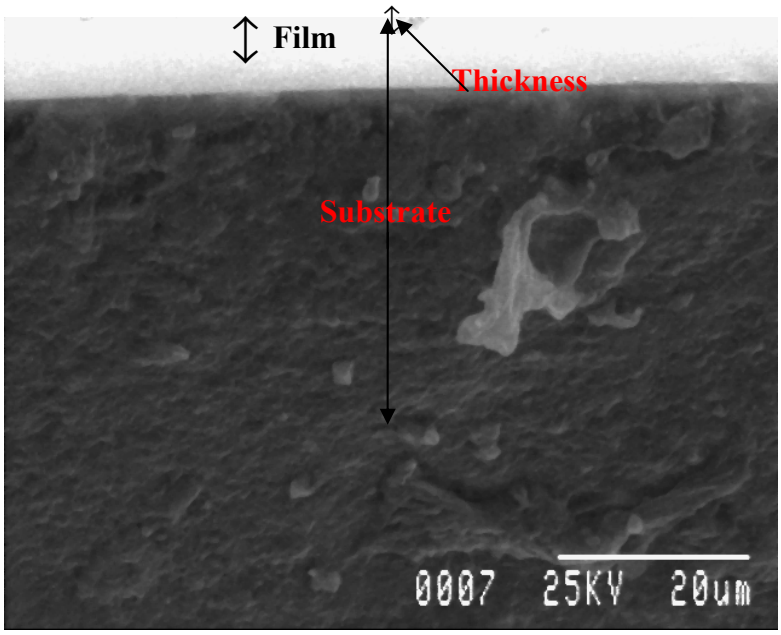

Figure 1. Cross-sectional SEM of ZnO film

3.2. Structural characterization and particle size analysis

Figure 2 shows the X-ray diffraction (XRD) patterns of the samples deposited on glass substrate. Figure 2 (a) to 2 (d) shows the spectra of the samples heat treated at 200^{o}C, 300^{o}C, 350^{o}C and 400^{o}C. The heat treatment was done in air for 2 hours. The materials were scanned in the range 20-60^{o}. The 2θ variation was employed with a 0.05 degrees step and a time step of 1 second. Intensity in arbitrary units is plotted against 2θ in figure 1. It is seen from figure 2 (a) that peaks appears at 31.714^{o}, 34.389^{o}, 36.205^{o}, 47.434^{o}and 56.576^{o}. The diffraction patterns reveal good crystalline quality without any appreciable changes from pure ZnO films and are genuinely polycrystalline with a hexagonal wurtzite structure. All the peaks are in good agreement with the Joint committee on powder diffraction standard (JCPDS) data belonging to hexagonal *ZnO* structure [14]. The corresponding reflecting planes are (100), (002), (101), (102) and (110) respectively. The XRD patterns of all the samples indicated enhanced intensities for the peaks corresponding to (002) plane, indicating preferred orientation along the c-axis.

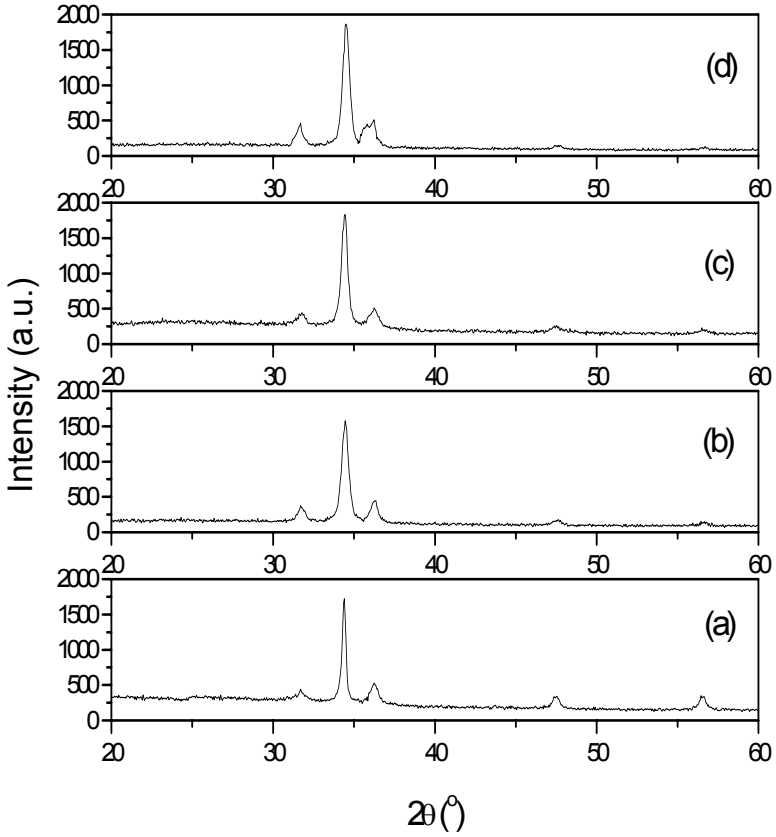

Figure 2. X-ray diffraction pattern of ZnO thin films heat treated at (a) 200°C, (b) 300°C, (c) 350°C and (d) 400°C

Quantitative information concerning the preferential crystal orientation can be obtained from the texture coefficient, *TC*, defined as [15-18]

$$TC(hkl) = \frac{I(hkl)/I_o(hkl)}{\left(1/n\right)\sum_n I(hkl)/I_o(hkl)}$$

where $TC(hkl)$ is the texture coefficient, n is the number of diffraction peaks considered, $I(hkl)$ is the measured x-ray intensity and $I_o(hkl)$ is the corresponding recorded intensity according to JCPDS card [14]. $I_o(hkl)$ represents the x-ray intensities from standard ZnO powder with randomly oriented grains or with no preferred orientation [14]. Since three diffraction peaks were used ((100), (002), (101)), the maximum value $TC(hkl)$ possible is 3. The variations of $TC(hkl)$ for (002) peak film is presented in Figure 3. The texture coefficient for the (002) orientation has been found to increase from 2.247 to 2.291 as the annealing

temperature is increased from 200°C to 300°C. No significant change is found with further heat treatment. The value of the texture coefficient indicates the maximum preferred orientation of the films along the diffraction plane, meaning that the increase in preferred orientation is associated with increase in the number of grains along that plane. Thus, in the present investigation, with increase in annealing temperature, the crystallinity along (002) plane improves upto 300°C and finally saturates.

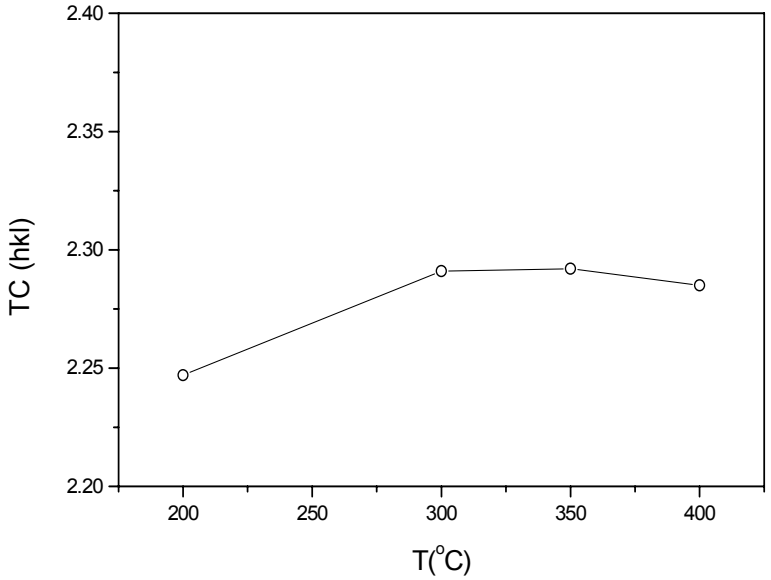

Figure 3. Variation of TC(hkl) values of the (002) peak of ZnO films with temperature

The value of $TC(002)$ for films deposited from sodium zincate bath as cationic precursor and hot water as anionic precursor was 1.948 (X-ray patterns not shown here for brevity). The pH and concentration of the sodium zincate bath was optimized at 13.20 ± 0.05 and 0.1M respectively [9]. The value of $TC(002)$ for films deposited from 0.1M zinc chloride solution at room temperature as cationic precursor and 0.075M sodium hydroxide at 70°C as anionic precursor was 1.825. All the films were heat treated at 350°C. The pH the cationic and anionic precursor was optimized at 4.70 and 11.10 respectively [19].

Utilizing the X-ray diffraction data, the average particle size was estimated from Williamson-Hall equation [20-21]

$$\beta \cos\theta = \frac{k\lambda}{D} + 4\varepsilon \sin\theta$$

where λ is the wave length of radiation used (1.5418Å for CuK_α radiation used), k is the Scherrer constant, β is the full width at half maximum (FWHM) intensity of the diffraction peak for which the particle size is to be calculated, θ is the

diffraction angle of the concerned diffraction peak, D is the crystallite dimension (or particle size) and ε is the lattice strain. In general the experimentally observed broadening (β_o) is the total contribution from particle size and strain broadening (β) and instrumental broadening (β_i). Thus the broadening due to size and strain (β) can be obtained from the experimentally observed broadening (β_o) using the equation [22]:

$$\beta = \beta_o - \beta_i$$

Diffraction data from standard silicon (Si) powder was used to measure the instrumental broadening [23-24]. The broadening (in FWHM) against 2θ obtained for standard silicon sample was plotted in a graph and was used as reference. The instrumental broadening at the observed peak positions for ZnO was evaluated from the graph.

X-ray line broadening analysis to evaluate FWHM (β) was carried out using computer software MARQ2 [9, 25-26]. The software utilizes Marquardt least-squares procedure for minimizing the difference between the observed and simulated diffraction patterns. The peak-shape and intensity of reflection is modeled with a pseudo-Voigt (pV) analytical function, which is a combination of a Gaussian and a Lorentzian functions representing lattice strain broadening and crystallite size broadening respectively. The background intensity is subtracted by fitting the background with a suitable linear function. A typical plot of MARQ2 analysis for ZnO sample heated at 350°C is shown in Figure 4. The dotted curve represents the experimental intensity data (I_o) and the continuous curve represents the calculated (simulated) intensity data (I_c). The difference plot $(I_c - I_o)$ is shown at the bottom.

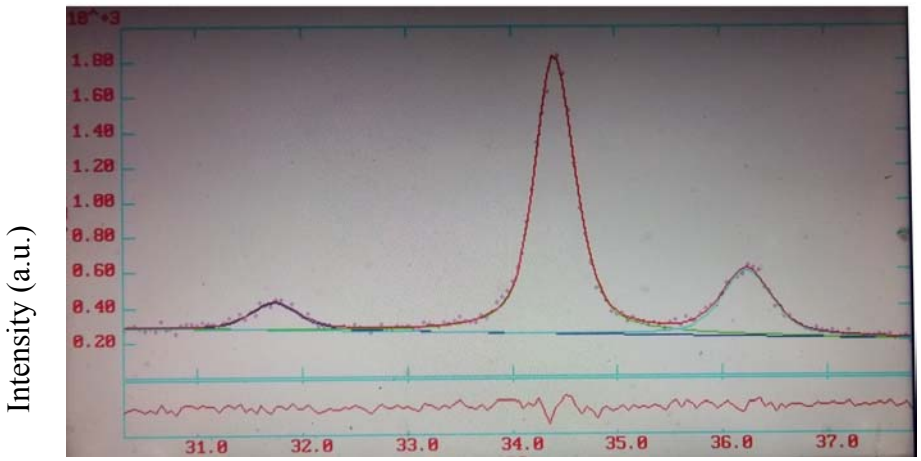

Figure 4. Observed (dotted) and simulated (continuous) XRD patterns of ZnO thin film heated at 350°C

From the values of β_o obtained using MARQ2 fitting and the corresponding values of instrumental broadening β_i, FWHM β was calculated using equation 2. Figure 5 shows the plot of $\beta\cos\theta$ against $4\sin\theta$ (Williamson-Hall plots or W-H plots). The slope of the plots represents average strain in the films whereas the inverse of intercept on $\beta\cos\theta$ axis gives the crystallite size (D) according to equation 1. The particle size was evaluated using $k = 0.9$, which corresponds to spherical crystallites and $\lambda = 1.5418$ Å, the wavelength of CuK_α radiation. The average value of particle size for pure ZnO is 22.75 nm. The strain in the film was 2.04×10^{-3}.

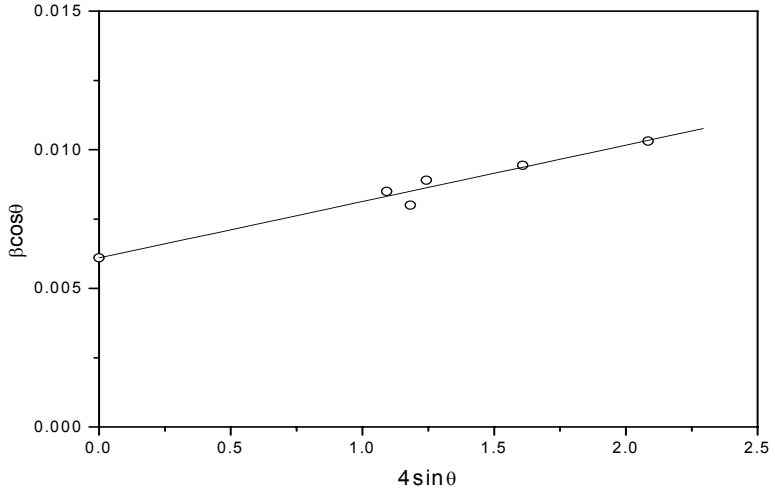

Figure 5. Williamson-Hall plot of ZnO film

Figure 6 shows the TEM micrograph of ZnO powder scratched out form the film. Particle sizes ranging between 23 to 28 nm was observed in the TEM image with an average value of 25.8 nm. Figure 7 shows the HRSEM micrograph of pure ZnO film prepared from zinc chloride solution as cationic precursor sodium hydroxide as anionic precursor. HRSEM study at normal incidence was undertaken in a FEI FEG Nova 600 Nanolab at 5 kV. The image with magnification $\times10000$ reveals structure consisting of many spheroid-like nano particles with an average size of ~31.2 nm. The histogram of particle size distribution is shown in figure 8. Figure 9 on the other hand shows the TEM image of ZnO film deposited from sodium zincate complex as cationic precursor. An average particle size of ~41nm was observed from TEM measurements. All the films were heat treated at 350^{o}C prior to measurements.

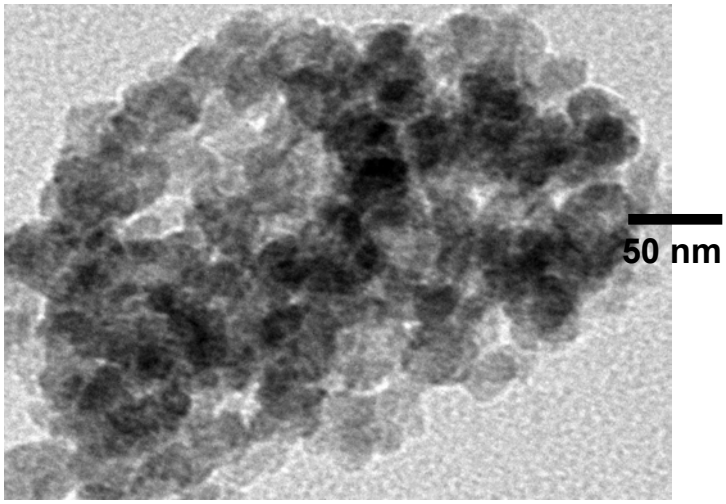

Figure 6. TEM image of ZnO prepared from ammonium zinacte bath

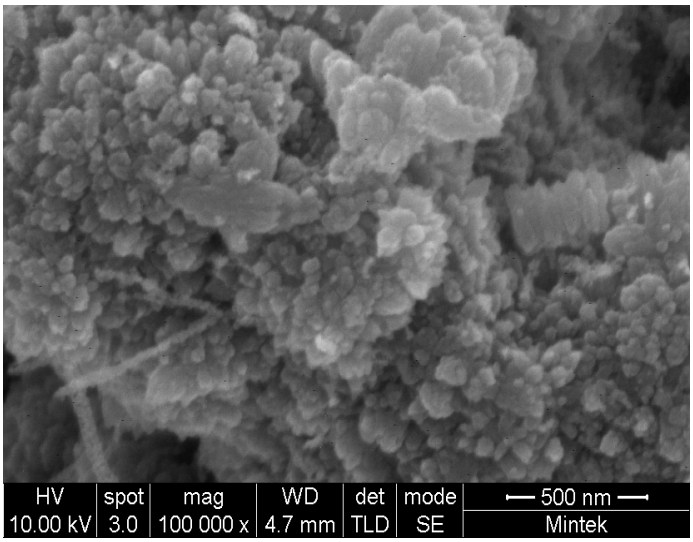

Figure 7. HRSEM image of ZnO prepared from zinc chloride precursor

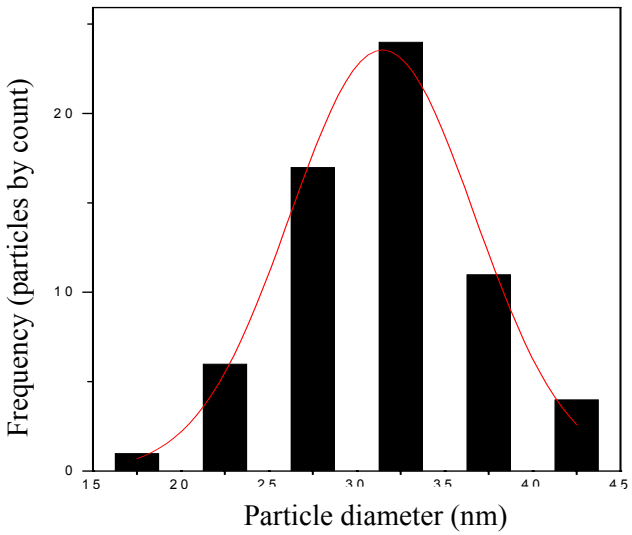

Figure 8. Histogram of particle size distribution

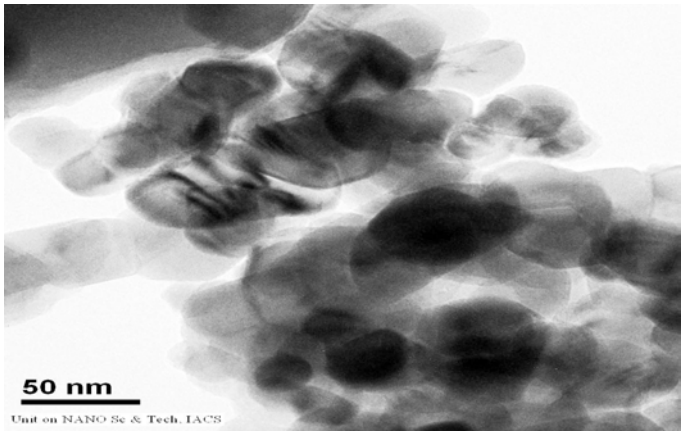

Figure 9. TEM image of ZnO prepared from sodium zincate complex

Figure 10 shows EDX analysis of the ZnO thin film heat treated at 350^{o}C. EDX indicates that the products consist of zinc and oxygen elements. The silicon signal appears from the substrate and the level of silicon contamination detected in the films deposited is ~1 at.%. No other impurity was detected in the films. Films deposited from sodium containing complex always introduces the possibility of highly mobile sodium ions in the films [13].

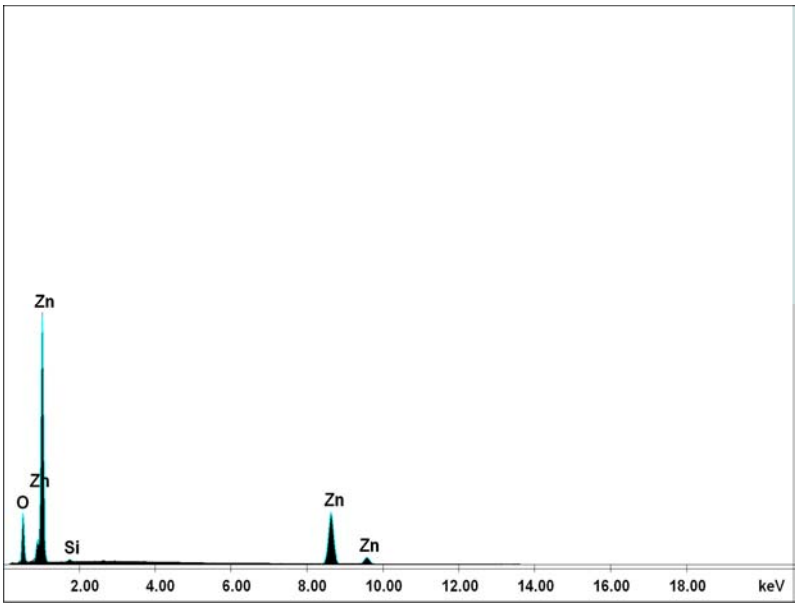

Figure 10. EDX spectrum of ZnO

FTIR spectroscopy is very useful tools for investigating vibrational properties of synthesized materials. The band positions and absorption peak not only depend on the chemical composition and structure of the thin films but on the morphology of thin films also. FTIR analysis was performed using Perkin-Elmer FTIR [FTIR spectrum RX1]. The FTIR spectrum of ZnO heat treated at 250^{o}C is shown in Figure 11. The absorption band observed at 483.4cm^{-1} is attributed to the ZnO stretching vibrations [27-29].

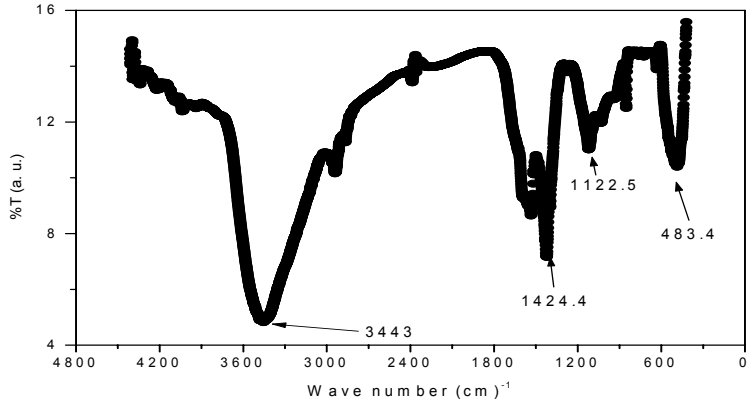

Figure 11. FTIR spectrum of ZnO

The band at 1424.4 cm^{-1} may be attributed to C-O stretching frequencies [30] and the band at 3443 may be attributed to O-H species in the film [30-31]. The band at 1122.5 could not be ambiguously assigned. It may be due to weakly bound acetic acid molecule [30].

The results of the present investigation showed that films obtained from ammonium zincate complex exhibits highest c-axis orientation and least crystallite size. Use of ammonium zincate complex avoids the possibility of highly mobile sodium ions in the deposited films. From physical appearance of the films it also appears that films with best homogeneity and smoothness are obtained for ammonium complex.

4. Conclusions

An analysis of the results presented here indicates that strongly c-axis oriented polycrystalline ZnO films can be prepared by SILAR technique from ammonium zincate bath prepared from zinc acetate as the staring precursor. The film growth rate is a very sensitive function of zincate bath pH. The films produced are strongly adherent and mechanically hard if pH is properly optimized. The pH has been optimized in the range 10.75-10.85 for ammonium zincate bath. Clearly, if the deposition conditions are not optimum, one can get powdery and non-adherent. The films are phase pure containing no other impurities as revealed from EDX. The average particle size estimated by x-ray line broadening method was found to be 22.75 nm which agrees well with TEM value of 25.8 nm. This is on the lower side compared to those obtained from sodium zincate as starting precursor(~41 nm) and zinc chloride complex (~ 31.2 nm). The value of texture coefficient is ~2.29 for films deposited from ammonium zincate complex and is on the higher side for films synthesized from other zinc complexes. The porosity in the films estimated by cross-sectional SEM was ~32%. FTIR spectrum reveals the presence of ZnO stretching vibration.

Acknowledgement

The authors are grateful to Dr. Rajarshi Ghosh, Dept. of Chemistry, The University of Burdwan for recording the FTIR spectrum. One of the authors (PM) gratefully acknowledges CSIR (Council of Scientific and Industrial research, New Delhi, India) for providing some financial support for carrying out the work in the form of a research project [No. 03 (1195)/11/EMR-II].

REFERENCES

1. T. Negami, Y. Hashimoto and S. Nishiwaki, "$Cu(In,Ga)Se_2$ thin-film solar cells with an efficiency of 18%", Solar Energy Materials & Solar Cells, 67, 331 (2001).

2. K. V. Gurav, V. J. Fulari, U. M Patil, C. D. Lokhande and O. Joo, "Room temperature soft chemical route for nanofibrous wurtzite ZnO thin film synthesis", Appl. Surf. Sci., **256**, 2680 (2010).
3. F. Yakuphanoglu, Y. Caglar, S. Ilican and M. Caglar, "The effects of fluorin on the structural, surface morphologyand optical properties of ZnO thin films", Physica, **B 394**, 86 (2007).
4. M. Ristov, G. J. Sinadinovski, I. Grozdanov and M. Mitreski, "Chemical deposition of ZnO films", Thin Solid Films, **149**, 65 (1987).
5. Y. F. Nicolau and J. C. Menard, "Growth of ZnS, CdS and ZnO thin films by SILAR", J. Cryst. Growth, **92**, 128 (1988).
6. A. E. Rakhshani, "Al-doped zinc oxide films grown by successive chemical solution deposition", Appl. Phys., **A92**, 413 (2008).
7. A. E. Jimenez-Gonzalez and P. K. Nair, "Photosensitive ZnO thin films prepared by the chemical deposition method SlLAR", Semicond. Sci. Techol.,**10**, 1277 (1995).
8. P. Mitra and J. Khan, "Chemical deposition ZnO films from ammonium zincate bath", Mat. Chem. Phys., **98**, 279 (2006).
9. S. Mondal and P. Mitra, "Preparation of cadmium doped ZnO thin films by SILAR and their characterization", Bull. Mat. Sc., **35**, 751 (2012).
10. A. Wojcik, M. Godlewski, E. Guziewicz, R. Minikayev and W. Paszkowicz, "Controlling of preferential growth mode of ZnO thin films grown by atomic layer deposition", J. Crystal Growth, **310**, 284 (2008).
11. M. C. Sneed and R. C. Brasted, Comprehensive Inorganic Chemistry, Vol. 4, Princeton, New York, 1955.
12. S. S. Kale, R. S. Mane, H. M. Pathan, A. V. Shaikh, O. S. Joo and S. H. Han, "Preparation and characterization of ZnTe thin films by SILAR method Applied", Surface Science, **253**, 4335 (2007).
13. S. Mondal, K. P Kanta and P. Mitra, 'Preparation of ZnO film on p-Si and I-V Characteristics of p-Si/n-ZnO', Mat. Res., **15** (2012) doi.org/10.1590/S1516-14392012005000149
14. B. Post, S. Weissmann and H F McMurdie H F (eds.), Joint Committee on Powder Diffraction standards, Inorganic Vol., Card No. 36-1451, International Centre for Diffraction Data, Swarthmore, PA, 1990.
15. S. Ilican, Y. Caglar and M. Caglar, "Preparation and characterization of ZnO thin films deposited by sol-gel spin coating method", J. Opt. and Adv. Materials, **10**, 2578 (2008).
16. J. I. Pankove, Optical Processes in Semiconductors, Prentice-Hall Inc., Englewoord Cliffs, NJ, 1971.
17. C. S. Prajapati and P. P. Sahay, 'Growth, structure and optical characterization of Al-doped ZnO nanoparticle thin films', Cryst. Res. Technol., **46**, 1086 (2011).
18. C. Agashe, M. G. Takawale, B. R. Marathe and V. G. Bhide, "Structural properties of SnO_2: F films deposited by spray pyrolysis", Sol. Energy Mater., **17**, 99 (1988).
19. S. Mondal and P. Mitra, "Effect of Manganese Incorporation in ZnO Thin Films Prepared by SILAR", Sci. & Soc., **10**, 139 (2012).

20. T. Ungar and A. Borbely, "The effect of dislocation contrast on X-ray line broadening: a new approach to line profile analysis", Appl. Phys. Lett., **69**, 3173 (1996).
21. N. Choudhury and B. K. Sarma, "Structural characterization of lead sulfide thin films by means of X-ray line profile analysis", Bull. Mat. Sc., **32**, 43 (2009).
22. H. P. Klug and L. E. Alexander, X-ray diffraction procedures for polycrystalline and amorphous materials, 2nd edition, Wiley, New York, 1974.
23. S. Patra, P. Mitra and S. K. Pradhan, "Preparation of nanodimensional CdS by chemical dipping technique and their characterization", Materials Research, **14**, 17 (2011).
24. P. Sharma, A. Gupta, K. V. Rao, F. J. Owens, R. Sharma, R. Ahuja, J. M. O. Gullen, B. Johansson and G. A. Gehring, "Ferromagnetism above room temperature in bulk and transparent thin films of Mn-doped ZnO", Nature Material, **2**, 673 (2003).
25. X. Jumin and J. Wang, "Nanocrystalline Si3N4 with Si–C–N shell structure", Mater. Lett., **49**, 318 (2001).
26. B. Ghosh, H. Dutta and S. K. Pradhan, "Microstructure characterization of nanocrystalline Ni3C synthesized by high energy ball milling", Journal of Alloys and Compounds, **479**, 193 (2009).
27. Z. Yang, Z. Ye, Z. Xu and B. H. Zhao, "Effect of the Morphology on the P Optical Properties of ZnO Nanostructured", Physica, **E 42**, 116 (2009).
28. T. Ivanova, A. Harizanova, T. Koutzarova and B. Vertruyen, "Study of ZnO solgel films: Study of ZnO solgel films: Effect of annealing", Materials Letters, **64**, 1147 (2010).
29. Z. R. Khan, M. S. Khan, Zulfequar and M. S. Khan, "Optical and Structural Properties of ZnO Thin Films fabricated by Sol-Gel Method", Materials Sciences and Applications, **2,** 340 (2011).
30. M. N. Kamalasanan and S. Chandra, "Sol-gel synthesis of ZnO thin films", Thin Solid Films, **288,** 112 (1996).
31. A. Pakdel and F. E. Ghodsi, "Influence of drying conditions on the optical and structural properties of sol-gel derived ZnO nanocrystalline films", Pramana-J. Phys., **76,** 973 (2011).